Neurobiology of Disease

The Gliopeptide ODN, a Ligand for the Benzodiazepine Site of $GABA_A$ Receptors, Boosts Functional Recovery after Stroke

Rhita Lamtahri,[1] Mahmoud Hazime,[1] Emma K. Gowing,[2] Raghavendra Y. Nagaraja,[2] Julie Maucotel,[3] Michael Alasoadura,[1] Pascale P. Quilichini,[4] Katia Lehongre,[5] Benjamin Lefranc,[1,6] Katarzyna Gach-Janczak,[1,7] Ann-Britt Marcher,[8] Susanne Mandrup,[8] David Vaudry,[1,6] Andrew N. Clarkson,[2]* Jérôme Leprince,[1,6]* and Julien Chuquet[1]*

[1]Normandie Université, UNIROUEN, Institut National de la Santé et de la Recherche Médicale U1239, Neuronal and Neuroendocrine Differentiation and Communication, Rouen, France, [2]Department of Anatomy, Brain Health Research Centre and Brain Research New Zealand, University of Otago, Dunedin, 76000, 9054, New Zealand, [3]Normandie Université, UNIROUEN, Animal Facility, Rouen, 76000, France, [4]Aix Marseille Univ, INSERM, INS, Inst Neurosci Syst, 13005, Marseille, France, [5]Inserm U 1127, Centre National de la Recherche Scientifique Unite Mixte de Recherche 7225, Sorbonne Universités, UPMC Univ Paris 06 Unite Mixte de Recherche S 1127, Institut du Cerveau et de la Moelle épinière, ICM, Paris, F-75013, France, [6]Institute for Research and Innovation in Biomedicine, Normandie Université, PRIMACEN, Rouen, 76000, France, [7]Department of Biomolecular Chemistry, Medicinal University of Łódź, Łódź, 90-137, Poland, and [8]Department of Biochemistry and Molecular Biology, University of Southern Denmark, Odense, 5230, Denmark

Following stroke, the survival of neurons and their ability to reestablish connections is critical to functional recovery. This is strongly influenced by the balance between neuronal excitation and inhibition. In the acute phase of experimental stroke, lethal hyperexcitability can be attenuated by positive allosteric modulation of $GABA_A$ receptors ($GABA_A$Rs). Conversely, in the late phase, negative allosteric modulation of $GABA_A$R can correct the suboptimal excitability and improves both sensory and motor recovery. Here, we hypothesized that octadecaneuropeptide (ODN), an endogenous allosteric modulator of the $GABA_A$R synthesized by astrocytes, influences the outcome of ischemic brain tissue and subsequent functional recovery. We show that ODN boosts the excitability of cortical neurons, which makes it deleterious in the acute phase of stroke. However, if delivered after day 3, ODN is safe and improves motor recovery over the following month in two different paradigms of experimental stroke in mice. Furthermore, we bring evidence that, during the subacute period after stroke, the repairing cortex can be treated with ODN by means of a single hydrogel deposit into the stroke cavity.

Key words: **endozepine; inhibition; peptide; peri-infarct; recovery; stroke**

Significance Statement

Stroke remains a devastating clinical challenge because there is no efficient therapy to either minimize neuronal death with neuroprotective drugs or to enhance spontaneous recovery with neurorepair drugs. Around the brain damage, the peri-infarct cortex can be viewed as a reservoir of plasticity. However, the potential of wiring new circuits in these areas is restrained by a chronic excess of GABAergic inhibition. Here we show that an astrocyte-derived peptide, can be used as a delayed treatment, to safely correct cortical excitability and facilitate sensorimotor recovery after stroke.

Received Aug. 27, 2020; revised Dec. 14, 2020; accepted Mar. 25, 2021.

Author contributions: R.L., M.H., E.K.G., R.Y.N., J.M., M.A., K.G.-J., A.N.C., and J.C. performed research; R.L., M.H., E.K.G., R.Y.N., J.M., M.A., P.P.Q., K.L., A.N.C., and J.C. analyzed data; P.P.Q., K.L., D.V., A.N.C., and J.C. designed research; P.P.Q., D.V., and J.L. edited the paper; B.L., A.-B.M., S.M., and J.L. contributed unpublished reagents/analytic tools; A.N.C. and J.C. wrote the paper; J.C. wrote the first draft of the paper.

This work was supported by Institut National de la Santé et de la Recherche Médicale U1239; Fondation AVC sous égide de la Fondation pour la Recherche Médicale et ses partenaires, Grant FRAVC1180713009 to J.C., Normandy Region and the European Union; Europe gets involved in Normandy with European Regional Development Fund, a Grant Interreg TC2N to D.V.; New Zealand Neurological Foundation; Royal Society of New Zealand Project Grant; Ministry of Business, Innovation and Employment, New Zealand; Brain Research New Zealand animal costs; and New Zealand Lottery Health equipment grant. We thank Dr Arnaud Arabo who provided help and expertise that greatly assisted the research.

*A.N.C., J.L., and J.C. contributed equally to this work.

The authors declare no competing financial interests.

Correspondence should be addressed to Julien Chuquet at julien.chuquet@univ-rouen.fr.

https://doi.org/10.1523/JNEUROSCI.2255-20.2021

Introduction

Stroke remains a devastating clinical challenge because there is no efficient therapy to either minimize neuronal death with neuroprotective drugs or to enhance spontaneous recovery with neurorepair drugs. The chronic and ever-changing balance between neuronal excitation and inhibition is a primary trigger for the initial stroke progression as well as the impairment in the ability to regain function. Given its predominant role in the control of inhibition, GABAergic transmission is a major target to act on the dynamic of this balance (Bachtiar and Stagg, 2014; Roux and Buzsáki, 2015). The use of pharmacological manipulations targeting $GABA_A$ receptors ($GABA_A$Rs) to modify the course of ischemic cell damage and their sequelae is an old quest: numerous preclinical experiments have demonstrated that

sustaining GABA neurotransmission to counteract the initial excitotoxic effect of glutamate released minutes to hours after the onset of stroke can afford protection (Sydserff et al., 1995; Shuaib and Kanthan, 1997; Green et al., 2000; Schwartz-Bloom and Sah, 2001; Marshall et al., 2003). In this respect, benzodiazepines with positive allosteric modulation profile were repeatedly shown to be neuroprotective after cerebral ischemia (Schwartz et al., 1994, 1995; Schwartz-Bloom et al., 1998; Galeffi et al., 2000). However, like all neuroprotective drug therapies to date, positive GABA modulators have failed to translate into clinical use.

In recent years, GABA modulation in stroke has been revitalized with the understanding that, once the infarction is consolidated, the excitation and inhibition balance switches from hyperexcitability to hypoexcitability in the peri-infarct cortex, because of a loss of the astroglial GABA tranporter, GAT3, and resultant excess in ambient GABA (Clarkson et al., 2010; Carmichael, 2012). This prolonged synaptic depression is thought to limit neuronal circuit reorganization and therefore the regain of sensorimotor functions (Hummel et al., 2009; Kim et al., 2014). Dampening the stroke-induced elevation in inhibition using a negative allosteric modulator (NAM) targeting the benzodiazepine site of $GABA_AR$, enhances sensorimotor recovery in mice and rats (Clarkson et al., 2010, 2015; Lake et al., 2015; Alia et al., 2016; Orfila et al., 2019).

Endozepines, known as the endogenous ligands of benzodiazepine-binding sites, comprise the diazepam binding inhibitor (DBI, also known as acyl-CoA binding protein [ACBP]) and its processing products, including the octadecaneuropeptide (ODN), a small peptide of 18 amino acids (DBI_{33-50}) (Tonon et al., 2020). In the brain, DBI is one of the major proteins expressed and released by astrocytes but not by neurons (Loomis et al., 2010; Tonon et al., 2020). DBI and ODN bind to the benzodiazepine site of the $GABA_AR$ where they act as allosteric neuromodulators (Bormann, 1991; Barmack et al., 2004; Qian et al., 2008; Möhler, 2014; Dumitru et al., 2017). Point mutation targeting the benzodiazepine site of $GABA_AR$ renders neuronal cells insensitive to ODN (Dumitru et al., 2017). At micromolar concentrations, electrophysiological studies show that ODN acts as a NAM on $GABA_ARs$, that is, reduces $GABA_AR$-mediated inhibition (Guidotti et al., 1983; Ferrero et al., 1986; Barmack et al., 2004; Alfonso et al., 2012; Dumitru et al., 2017) with no epileptogenic effect (Vezzani et al., 1991). ODN appears to be a relatively new astroglial modulator of $GABA_AR$ signaling and should therefore be considered for its potential to correct the imbalance between excitation and inhibition that arises as a consequence of a stroke. Here, we tested the gliopeptide ODN for its potency to enhance recovery after stroke. We show that ODN boosts the excitability of cortical neurons, which makes it deleterious in the acute phase of stroke. However, if delivered 3 days after the stroke onset, ODN is safe and improves motor recovery in two different models of focal brain ischemia. Furthermore, we bring novel evidence that, during the subacute period after stroke, the repairing cortex can be treated with ODN by the means of a single hydrogel injection into the infarct cavity allowing for direct targeting of the peri-infarct cortex.

Materials and Methods

Animals and approvals

Eight- to 12-week-old (20-25 g) male C57BL/6J mice were purchased from Janvier Laboratories. ACBP KO ($ACBP^{-/-}$ hereinafter referred to as $DBI^{-/-}$) mice were obtained from Prof. Mandrup Laboratory (University of Southern Denmark). Mice were backcrossed to the C57BL/6J Bom Tac strain for 10 generations to obtain a congenic background as previously described (Neess et al., 2011). WT ($DBI^{+/+}$) and KO ($DBI^{-/-}$) were littermate generated from heterozygote mice. The homozygote $DBI^{-/-}$ mice used in this study were identified by genotyping PCR. Aged female (20 ± 2 months) mice were obtained from the Hercus Taieri Resource Unit at the University of Otago. Experiments, approved by the Ethics Committee for Animal Research of Normandy or the University of Otago Animal Ethics Committee, were conducted by authorized investigators in accordance with the recommendations of the European Communities 86/609/EEC. All procedures were undertaken and reporting done in accordance to the ARRIVE (Animal Research: Reporting *In Vivo* Experiments) guidelines. All *in vivo* procedures were conducted between 8:00 A.M. to 6:00 P.M. in specific experimental rooms.

In vivo *electrophysiology*

Under isoflurane anesthesia (2%-2.5%), two holes were drilled over the whisker barrel cortex with the dura mater intact, and two glass micropipettes were inserted for recording and micro-injection. After the surgical procedure, isoflurane was reduced to 1.1 ± 0.1% for a 30–45 min resting period. All *in vivo* recordings were done with an amplifier PowerLab 8/35 and aquired with Labchart software (AD-Instrument).

Local field potential (LFP) and extracellular unit recording (EU). An aCSF-filled glass-micropipette/AgCl/Ag electrode, 3- to 6-μm-diameter opening, was positioned in cortical layer 4 of the whisker barrel cortex. Reference and ground electrodes (AgCl/Ag wire) were inserted into the cerebellum. For ODN microinjection, a glass micropipette (10-μm-diameter opening) was placed 50–100 μm away from the recording pipette's tip. For KCl-induced spreading depolarization waves, 2 μl of KCl (0.5 mol/L) was slowly infused (10 min) at a distant site from the recording site (4 mm). The signal was bandpass filtered at 200–2000 Hz and digitized at 20 kHz for EU or at 1–100 Hz and digitized at 4 kHz for LFP. Signals were recorded for 12 min before the microinjection of 1 μg of ODN (0.5 μl) and compared with a 12 min period beginning 3 min after the microinjection ended (3 min). Spike detection and sorting were then performed semiautomatically, using Klusta software suite (Rossant et al., 2016), freely available (http://klusta-team.github.io). Spikes were identified from the high-frequency component by SpikeDetekt using a thresholding of 4.5 times the standard deviation of the signal. Clustering was performed using Klustakwik to verify the coherence of the clusters of the two periods (pre- vs post-injection period) and eliminate spikes that are an apparent noise (<1% of total spikes). Waveforms were viewed and extracted using Phy graphical unit interface. For each animal, the spiking change (%) represents a normalized difference of spikes between the pre- and the post-injection period.

Somatosensory-evoked potentials (SEPs). The left whiskers were stimulated with a short rod controlled by an Arduino UNO board at 0.1 Hz, 100 times. Signal was acquired at 4 kHz; and analysis was performed by a custom-made script in MATLAB, bandpass filtered (1-25 Hz), and segmented around each stimulation (−2 to 4 s). Each trial was normalized by subtracting the baseline i.e., signal average of the signal comprised between −1 and −0.1 s). For the SEP slope, 100 trials were superimposed and averaged, and the initial deflection of the LFP was defined as the interval within 20%-80% of the peak-to-peak amplitude. The slope was computed by linear regression of the selected region.

Intravital calcium imaging

A cranial window was made over the somatosensory cortex as previously described (Chuquet et al., 2010). Imaging was performed under anesthesia using 2-photon laser scanning microscope (SP8, Leica Microsystems). SR-101 (1 μM applied on the cortex for 10 min) and OGB1-AM (1.2 μg in 1 μl micro-injected in the cortex) were both excited at 805 nm. Frames (256 × 256 pixels) were collected at 3 Hz. *x-y* drifts were automatically corrected. All traces were median filtered. Signal was expressed as relative OGB1-AM fluorescence changes (dF/F_0) where F_0 is the mean of the lowest 20% of the somatic fluorescence signals. Astrocytic calcium surges were defined as transient increase of dF/F_0 signal exceeding 3 SDs.

Stroke models

Middle cerebral artery occlusion. Temporary focal cerebral ischemia was induced under general anesthesia (isoflurane 1.5%-2%) by occlusion of the right middle cerebral artery (MCAO) using the intraluminal

filament technique. Briefly, a nylon thread (80 μm in diameter) with a distal cylinder (1.5 mm and 180 μm in diameter) was inserted into the common carotid artery, advanced to the origin of the MCA (exept for sham), and removed 60 min later to allow reperfusion. A laser-Doppler flowmetry probe (Moor Instruments) was used to continuously monitor cerebral blood flow (CBF). Post-surgery analgesic care comprised intradermal ropivacaine (25 μl at 2.5 mg/ml, Naropeine) around sutures and applications of lidocaine/prilocaine cream (2.5% EMLA, AstraZeneca). The animals were then allowed to recover and were killed at day 2 or 28 after MCAO.

Cortical photothrombosis. Focal stroke was induced in the left hemisphere using the photothrombosis method in aged (20 ± 2-month-old) female C57BL/6J mice weighing 35.8 ± 5.6 g (Clarkson et al., 2010, 2011, 2019). Briefly, under isoflurane anesthesia (2%-2.5% in O_2), mice were placed in a stereotactic apparatus and the skull was exposed. A cold light source (KL1500 LCD, Carl Zeiss) attached to a 40× objective giving a 2-mm-diameter illumination was positioned 1.5 mm lateral from bregma, and 0.2 ml of Rose Bengal solution (Sigma-Aldrich; 10 g/L in saline, i.p.) was administered. After 5 min, the brain was illuminated through the skull for 15 min. All animals were randomly assigned to a treatment group 5 d post-stroke, by an operator not undertaking behavioral, histologic, or immunohistochemical assessments. All assessments were conducted by observers blind to the treatment group.

NMDA-induced excitotoxic damage

In isoflurane-anesthetized mice, excitotoxic lesions were induced by NMDA micro-injection (20 nmol/0.5 μl) into the right striatum (2.5 mm lateral, −4.0 mm ventral, and −0.7 mm posterior to the bregma) infused at a rate of 0.2 μl/min. The lesion volume was quantified 48 h later.

Peptide synthesis and drug preparation

Mouse/rat ODN (H-Gln-Ala-Thr-Val-Gly-Asp-Val-Asn-Thr-Asp-Arg-Pro-Gly-Leu-Leu-Asp-Leu-Lys-OH) was synthesized as previously described (Leprince et al., 2001). Flumazenil, a selective antagonist of the benzodiazepine site of the $GABA_AR$, and NMDA were purchased from Sigma-Aldrich and dissolved in sterile HEPES buffer supplemented with KCl (2.5 mmol/L) and NaCl (145 mmol/L), pH 7.4, and DMSO (dilution 1:4) for flumazenil. ODN or its vehicle was infused over 5 min into the lateral ventricle (3 μl; −0.1 mm posterior, 0.8 mm lateral, −2.5 mm ventral to the bregma) or into the cisterna magna for the experiment conducted under the 2-photon microscope.

In vivo *dosing with hydrogel impregnated with ODN*

A hyaluronan/heparan sulfate proteoglycan biopolymer hydrogel (HyStem-C, BioTime) was used to locally deliver ODN, to the peri-infarct cortex as described previously (Clarkson et al., 2011; Houlton et al., 2019). In brief, ODN was added to the HyStem/Gelin-S mix (component 1 of hydrogel, glycosyl/gelin 1:1), followed by addition of Extralink (component 2 of hydrogel) in a 4:1 ratio. In prior studies, we have reliably shown that hydrogels can be used to release small and large proteins for at least 3 weeks from the stroke cavity (Li et al., 2010; Overman et al., 2012). Five days after stroke, 7.5 μl of HyStem-C, impregnated with either ODN (1 μg or 5 μg) or saline-vehicle, was injected directly into the stroke infarct cavity (30-gauge needle and a Hamilton syringe at coordinates 0 mm AP, 1.5 mm ML, and 0.75 mm DV).

Behavioral tests

MCAO. Behavioral tests were conducted by a manipulator blind to treatment groups. After a pretest performed 3 or 4 d before MCAO surgery, three sensorimotor tasks were conducted once a week.

The pole test was performed as described by Matsuura et al. (1997). Mice performed two different tasks: (1) mice were placed head upward on top of the vertical pole (55 cm). The time to turn completely head downward was measured (return task); and (2) the descent of the pole (descent task) was covered with Durapore tape (3M). The third test was the beam crossing test (Carter et al., 2001), measuring the time to cross a horizontal beam (diameter: 10 mm; length: 1 m). For animals unable to perform one of these three tasks, a time penalty of 60, 60, and 200 s was, respectively, attributed, corresponding to the worst performances (Mann and Chesselet, 2014).

Cortical photothrombosis. Recovery of forelimb motor function was determined by the cylinder and grid-walking tasks to assess their exploratory behavior and walking, respectively, as previously reported (Clarkson et al., 2010). Mice were tested ~7 d before stroke to establish a baseline performance level and then after 7, 14, 28, and 42 d post-stroke at approximately the same time each day. Observers blinded to the treatment group scored behaviors as previously described.

Immunofluorescent labeling of GFAP and infarct volume

Brains were sectioned, and every sixth section (30 μm thick) was collected and stored in cryopreservation solution. Slices were first incubated with a primary antibody (chicken anti-mouse GFAP, 1:3000, AB5541, Millipore) for 48 h at 4°C. Then, a secondary antibody (anti-chicken Alexa-488, 1:1000, SA5-10 071, Thermo Fisher Scientific), followed by the nuclear counterstain Hoechst (1:1000, Sigma-Aldrich), was used. Images were taken with an Olympus BX61 microscope. Changes in GFAP staining were investigated 2 and 6 weeks post-stroke, with measurements taken 0-200 μm and 800-1000 μm from the stroke border in layers 2/3 and 5, respectively. Using the software Fiji ImageJ (National Institutes of Health) the integrated density value was measured in all four ROIs.

Infarct volumes were determined 2 and 6 weeks post-stroke using cresyl violet staining and ImageJ analysis. The analysis is based on obtaining measurements from every sixth section, and infarct volume was quantified as follows: infarct volume (mm^3) = areas (mm^2) × (section thickness (mm) + section interval (mm)). Infarct volume was corrected for edema as described previously. All analyses were performed by an observer blind to the treatment groups.

Whole-cell voltage-clamp electrophysiological recordings

Mice (2- to 3-month-old) were anesthetized with isoflurane 3-7 d post-stroke or sham surgery, and brains were sliced and prepared for recordings of tonic currents. All recordings were made from peri-infarct pyramidal neurons within layer 2/3 of the primary motor cortex, as previously described (Clarkson et al., 2010, 2019). Neurons were voltage-clamped in whole-cell configuration using a MultiClamp-700B amplifier using microelectrodes (3-5 MΩ) filled with a cesium-methylsulfonate ($CsMeSO_4$)-based internal pipette solution. The recording aCSF was supplemented with 5 μM GABA to replenish the extracellular GABA concentration reduced by the high-flow perfusion of the slices.

Tonic inhibitory currents (I_{tonic}) were recorded as the reduction in baseline holding currents (I_{hold}) after bath-applying a saturating amount (100 μM) of the $GABA_AR$ antagonist SR-95 531 (gabazine), while voltage-clamping at 10 mV. ODN was added to the recording aCSF via perfusion, and their effects on I_{tonic} were recorded as the post-drug shift in I_{hold}. Drug perfusion continued until the shifting I_{hold} remained steady for 1-2 min.

Statistics

Sample size was calculated using the JavaScript utilities available at www.stat.ubc.ca/~rollin/stats/ssize/index.html with parameters determined from prior work. For experiments presented in Figures 1*A*, *D*, 2*B*, and 3*D*, the knowledge of the variability was too uncertain to reliably calculate a sample size (>80% power). For those experiments, we relied on reasonable assumptions to determine *a priori*, the number of animals used. Data are presented as mean ± SEM or as box-and-whisker plot showing the median (box = first and third quartiles; whisker = range). Statistics were performed using Prism software (GraphPad). Normal distribution of the datasets was tested by a Kolmogorov–Smirnov test. Pairwise means comparisons were performed using *t* test for normally distributed data, or Mann–Whitney test otherwise. For recovery studies, two-way ANOVA followed by *post hoc* Tukey's or Bonferroni's test for multiple comparisons was performed.

Data availability

All the data that support the findings of this study are available from the corresponding author.

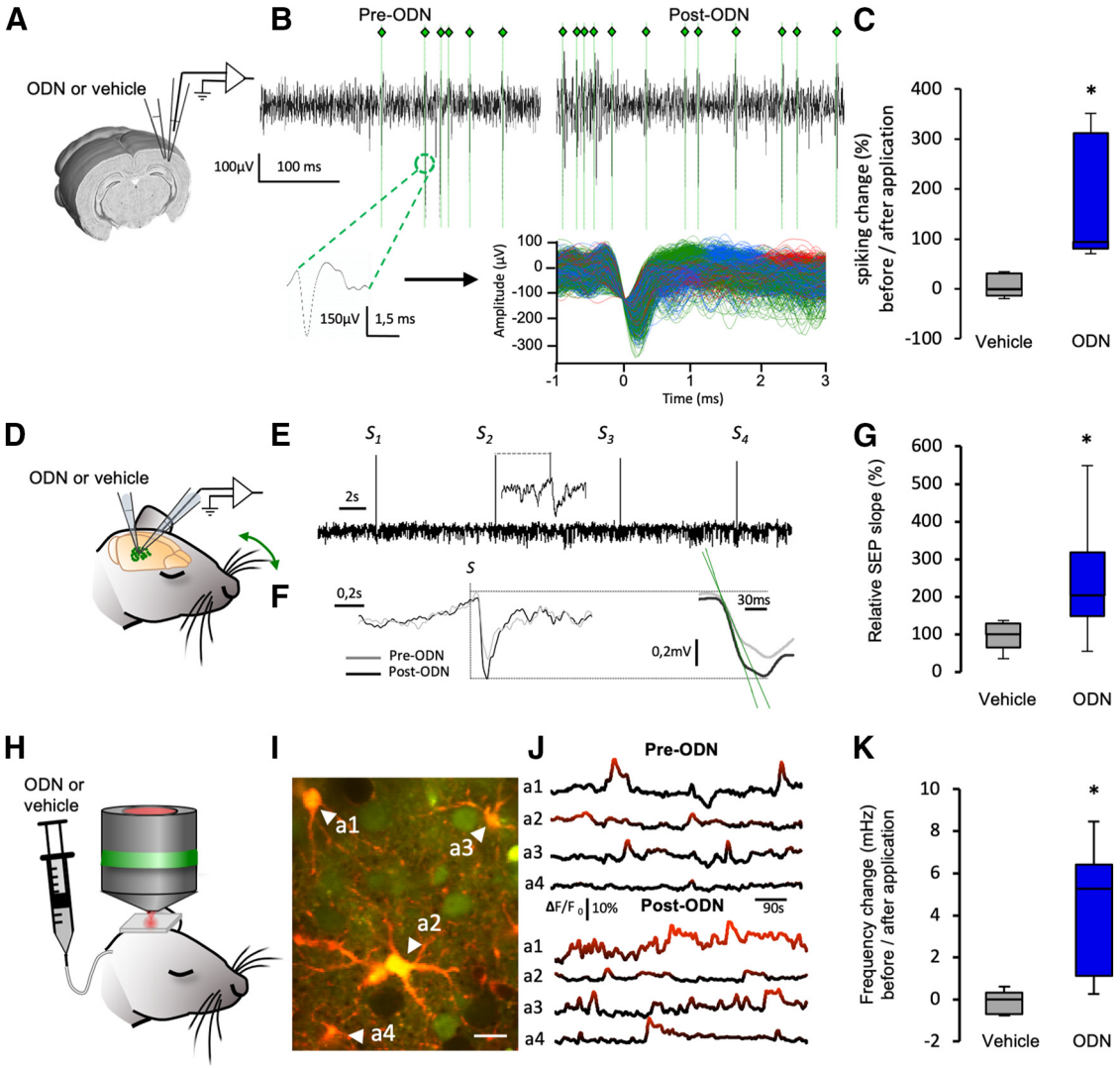

Figure 1. The gliopeptide ODN enhances neuronal and astrocytic activity in the cortex *in vivo*. ***A***, Experimental arrangement showing pipette positions for microinjection of ODN in the vicinity (~100 μm) of the recording pipette (layer 4). ***B***, Top, Representative EU recording trace comparing spontaneous neuronal spiking activity before and after ODN infusion (350 ms epoch). The post-treatment period recording started 6 min after the start of the infusion. Vertical green lines underneath the trace indicate the occurrence of spikes. Bottom, Representative examples of a detected spike (left) and a superimposed spike waveform showing 3 clusters of spikes (green, red, and blue). ***C***, The infusion of the vehicle solution did not change the number of spikes detected during the 12 min post-vehicle period ($p > 0.05$ vs 12 min pre-vehicle period, $n = 6$ mice). ODN significantly increased spiking ($p < 0.05$ vs pre-ODN period, $n = 6$ mice). ***D***, Experimental setup for SEP recorded in the whisker barrel cortex. The contralateral whisker pad was mechanically stimulated every 10 s evoking the typical negative shift of the LFP trace (***E***). ***F***, Representative SEP obtained after the average of 100 stimulations. ***G***, The SEP slope of the control group remained unchanged after the infusion of vehicle ($p > 0.05$, pre- vs post-treatment, $n = 6$ animals), whereas ODN treatment significantly increased the SEP slope ($p < 0.05$, pre- vs post-treatment, $n = 6$ animals). ***H***, Experimental setup for 2-photon imaging of astrocyte activity. ODN or its vehicle was administered by the cisterna magna route. ***I***, Astrocytes (white arrowheads) were double-labeled with Ca^{2+}-sensitive and Ca^{2+}-insensitive dyes (OGB-1 and SR-101, respectively). Scale bar, 10 μm. Depth: ~−250 μm. ***J***, Example of spontaneous somatic Ca^{2+} activity showing the occurrence of Ca^{2+} surges (red highlight). ***K***, The infusion of the vehicle did not change the frequency of astrocyte Ca^{2+} transients ($p > 0.05$ vs pre-vehicle period, $n = 5$ mice), whereas ODN significantly increased their frequency ($p < 0.05$ vs pre-ODN period, $n = 6$ mice). Data are represented as box-and-whisker plot (box = first and third quartiles; whisker = range). Mean values were compared using paired, two-tailed *t* test.

Results

Effect of ODN on cortical activity

Changes in neuronal excitation are critical for cell survival during the acute phase of stroke as well as for synaptic plasticity and recovery during the repair phase after stroke. To address the general hypothesis that extrinsic ODN can be used to safely manipulate neuronal excitability and influence postischemic repair, we first checked whether, as reported previously *in vitro*, ODN induced a measurable enhancement of cortical activity *in vivo*. In neuronal cell culture, the $GABA_AR$ NAM effect of ODN was observed in the micromolar to millimolar range (Guidotti et al., 1983; Ferrero et al., 1986; Alfonso et al., 2012). We therefore targeted this range to test ODN *in vivo*. In isoflurane-anesthetized mice, we recorded the effect of 1 μg of ODN or its vehicle on neuronal spiking of layer 4 of the somatosensory cortex (Fig. 1*A*). Inspection of electrophysiological recordings did not reveal any aberrant oscillations or sharp events that would indicate epileptiform activity (Fig. 1*B*). ODN increased spontaneous neuronal firing (181.5 ± 61.6% increase compared with the pretreatment period; $p < 0.05$; $n = 6$ mice; vehicle: 4.7 ± 11.4%; $p > 0.05$; $n = 6$), whereas vehicle administration did not result in any significant change in spiking activity (Fig. 1*C*). To further examine the potential of ODN to boost neuronal excitability, the effect of ODN was also tested during a somatosensory stimulation. A single deflection of the whiskers pad triggered a SEP in layer 4 of the contralateral barrel cortex (Fig. 1*D*,*E*). As a result of ODN

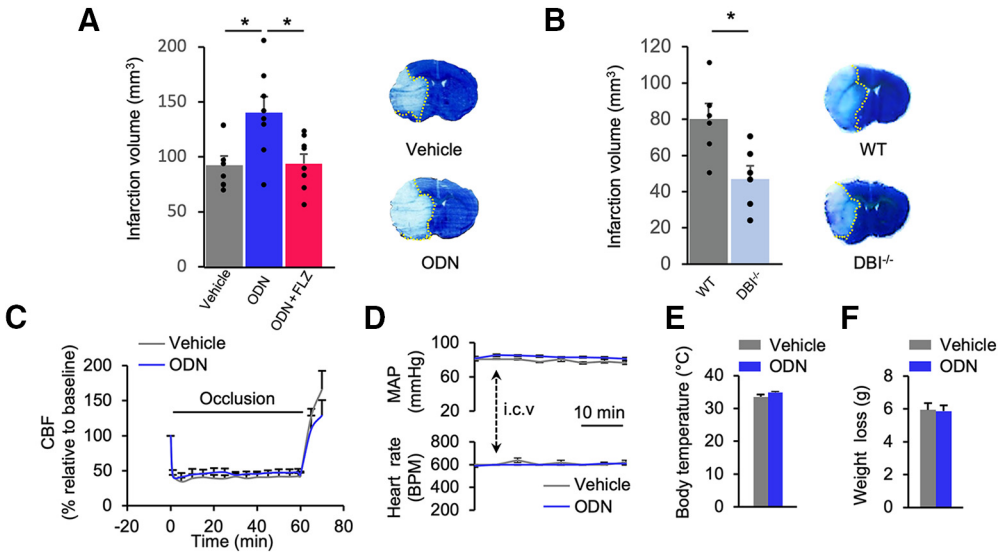

Figure 2. ODN exacerbates ischemic damages. ***A***, Average infarction volume when treatments are provided during the acute phase of focal cerebral ischemia, by intracerebroventricular injection. ODN significantly increased the volume of the lesion ($p < 0.05$ vs vehicle group; $n = 8$ animals/group). This effect was reversed by the selective $GABA_AR$ benzodiazepine site antagonist flumazenil (FLZ, $p > 0.05$ vs vehicle group, $n = 8$ animals). Right, Representative histologic analysis showing the infarction, unstained by thionine. ***B***, KO mice for DBI (*DBI*$^{-/-}$, the peptide precursor of ODN) were less vulnerable than WT mice to brain focal ischemia ($p < 0.05$ vs WT; $n = 6$ animals/group). Right, Representative lesions. ***C–F***, The exacerbation of the damage could not be attributed to a difference in the severity of cerebral blood flow decrease between groups during the procedure (***C***, $p > 0.05$ vs vehicle, $n = 8$ animals/group). Intracerebroventricular administration of ODN produced no effect on systemic physiological parameters (***D***), such as mean arterial pressure (MAP, $p > 0.05$) or heart rate (beats/min, $p > 0.05$ vs vehicle, vehicle $n = 3$; ODN $n = 4$), body temperature (***E***, $p > 0.05$ vs vehicle, $n = 8$/group), or post-stroke weight loss (***F***, $p > 0.05$ vs vehicle, $n = 8$/group). Data are mean ± SEM. Mean values were compared using unpaired, two-tailed Mann–Whitney test (***A***,***B***,***E***,***F***) followed by Bonferroni's *post hoc* testing for multiple comparison (***A***) or one-way ANOVA (***C***,***D***).

treatment, SEP slopes increased by 147.8 ± 71.8% showing that ODN increases neuronal excitability ($p < 0.05$ vs pretreatment period; $n = 6$ mice; vehicle group: 4.7 ± 26.4%; $p > 0.05$ vs pretreatment period; $n = 6$; Fig. 1*F*,*G*). Furthermore, the positive effect of ODN on cortical activity was also revealed by the increase of astrocytic network activity seen by intravital calcium imaging using a two-photon microscope (Fig. 1*H–J*). Astrocytes displayed spontaneous calcium transients at 3.6 ± 1.4 mHz during baseline as previously described (Chuquet et al., 2007). After ODN administration, transient frequency rose to 7.5 ± 0.8 mHz ($p < 0.05$; $n = 23$ cells from 6 animals), whereas calcium activity was unaffected following vehicle administration (3.1 ± 0.7 mHz vs 3.1 ± 0.8 mHz; $p > 0.05$; $n = 16$ cells from 5 animals; Fig. 1*J*,*K*). Overall, these results show, for the first time, that the endozepine ODN acts as an excitability-enhancer of the cerebral cortex *in vivo*.

Acute effect of ODN during cerebral ischemia

Within the first minutes to hours after stroke onset, depolarization and hyperexcitability are the primary culprits for the massive necrotic neuronal loss. Although ODN has a potent neuroprotective effect *in vitro* (Hamdi et al., 2011), enhancing cortical excitability in the acute phase of brain ischemia, when excitation is already lethal for neurons, may be inimical to cell survival. In order to examine whether the subtle changes of cortical activity elicited by ODN could influence ischemic neuronal death processes, we administered ODN (1 μg intracerebroventricular [i.c.v.]) during the acute phase of a focal brain ischemia elicited by intraluminal occlusion of the right middle cerebral artery (MCAO). The transient ischemia (60 min followed by reperfusion) produced a reproducible infarct 48 h later (Fig. 2*A*). Continuous laser Doppler flowmetry monitoring of the cerebral blood flow (CBF) confirmed that all animals underwent a similar ischemia and that ODN had no impact on residual CBF ($p > 0.05$ at any time point; Fig. 2*C*). The treatment with ODN resulted in a severe aggravation of the mean infarction volume (ODN group 140.35 ± 14.61 mm^3 vs vehicle group 92.32 ± 8.61 mm^3; $p < 0.05$; $n = 8$; Fig. 2*A*). Physiologic parameters well known to have a determinant impact on neuronal survival in stroke (arterial pressure, temperature, food intake) were not affected by central administration of ODN (Fig. 2*C–F*). Flumazenil, a selective antagonist of the benzodiazepine-binding site of the $GABA_AR$, fully reversed ODN-induced exacerbation (ODN+FLZ group 93.87 ± 8.70 mm^3 vs vehicle group 92.32 ± 8.61mm^3; $p > 0.05$; $n = 8$; Fig. 2*A*), confirming the involvement of the GABAergic signaling. MCAO was also conducted on KO mice for the DBI gene (*DBI*$^{-/-}$); and consistent with the above observations, DBI$^{-/-}$ animals appeared to be more resistant to MCAO than their WT counterparts (WT group 80.08 ± 8.73 mm^3 vs DBI$^{-/-}$ group 47.02 ± 7.30 mm^3; $p < 0.05$; $n = 6$; Fig. 2*B*). This result suggests that the endogenous production of the ODN precursor plays a role in the pathophysiology of stroke. In view of the above results, the most likely hypothesis for the ODN aggravated neuronal cell death is because of a decrease in GABAergic inhibition, a well-documented pathway in neuroprotection and recovery (Green et al., 2000; Clarkson et al., 2010). This was further corroborated by two other observations. First, we examined the effect of ODN in the case of a pure excitotoxic neuronal cell death induced by a microinjection of NMDA. The coadministration of ODN with NMDA significantly increased the size of the excitotoxic lesion (3.5 ± 0.4 mm^3 vs 6.4 ± 0.9 mm^3; $p < 0.05$; Fig. 3*A*,*B*). Second, another, albeit closely related pathophysiologic event, is spreading depressions, that is, waves of transient depolarization preceding cell damage in the compromised brain (Hartings et al., 2017). Local application of KCl on the healthy cortical tissue triggers such spreading depression events, as described previously (Chuquet et al., 2007). We found that central administration of ODN 10 min before the induction of a train of 2 or 3 spreading depressions, increased the number of events by 61.8% ($p < 0.05$ vs vehicle group; $n = 6$; Fig. 3*C*,*D*). The amplitude

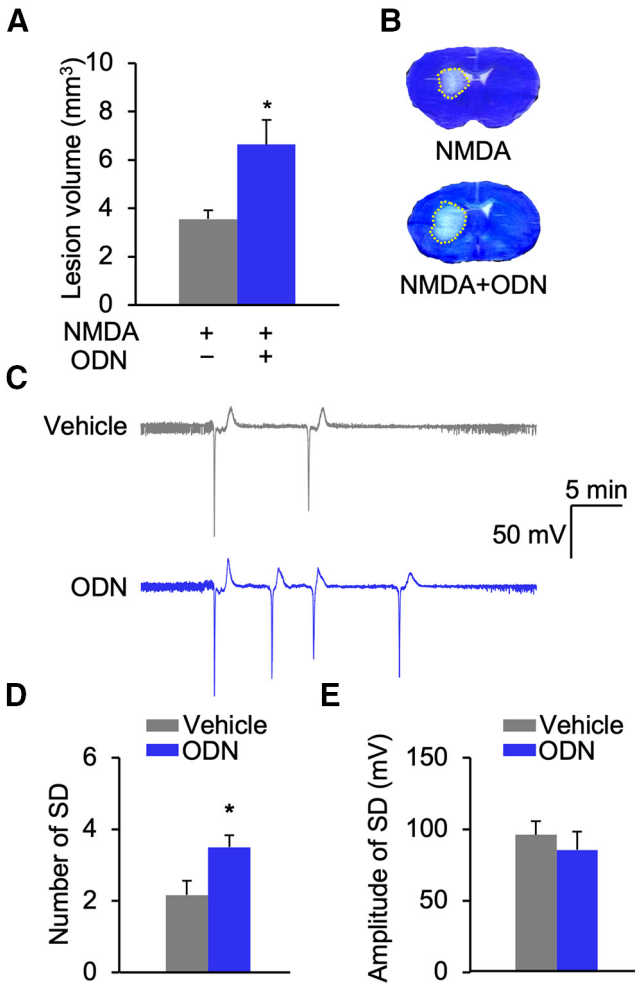

Figure 3. ODN enhances excitotoxicity and spreading depolarization waves. ***A***, NMDA-induced striatal damages were exacerbated by coadministration of the gliopeptide ODN ($p < 0.05$; NMDA, $n = 14$; and NMDA+ODN, $n = 13$). ***B***, Right, Representative lesions. ***C***, Intracortical infusion of KCl induced recurrent spreading depression (SD) waves: representative LFP traces showing the typical negative shift of spreading depressions, whose number was increased in the presence of ODN ($p < 0.05$, vehicle, $n = 6$; ODN, $n = 6$) while their amplitude remained unchanged (***D***,***E***; $p > 0.05$). Data are mean ± SEM. Mean values were compared using two-tailed Mann–Whitney test.

and temporal features of spreading depressions were unchanged by ODN ($p > 0.05$; $n = 6$; Fig. 3*E*). In a condition of hyperexcitability, such as the one observed during the acute phase of ischemia, the neuroprotective features of the gliopeptide ODN are surpassed by its pro-excitotoxic effect. Together, these observations are fully consistent with the view that the negative allosteric modulation of the $GABA_AR$ is not safe in the acute phase of stroke (Clarkson et al., 2010).

Effect of ODN on functional recovery after MCAO stroke

In the weeks following stroke, the peri-infarct surviving tissue is in a state of heightened neuronal plasticity, which is intended to promote the recovery of lost functions. Some of the repair processes that are altered rely on an increase in synaptic transmission and therefore depend on an optimal excitation/inhibition balance. Contrary to the acute phase of stroke (hours) where excitation must be decreased to maintain neuronal survival, in the chronic phase (weeks), an excess of GABAergic inhibition prevents optimal recovery (Clarkson et al., 2010). Spurred by recent studies demonstrating that the exogenous benzodiazepine inverse agonist L655,708 is efficient in correcting this imbalance and improving the recovery of mice after stroke (Clarkson et al., 2010; Lake et al., 2015), we made a similar hypothesis that chronic treatment with the endozepine ODN would promote enhanced neuronal plasticity. To avoid any interactions of ODN with its effects on cell death during the acute phase of stroke, we began the treatment with the gliopeptide (or its vehicle) 72 h after the onset of stroke (Fig. 4*A*,*B*), a sufficient delay for the lesion to be fully formed and no further expansion observed beyond this period. Preoperative performances in the "latency to turn" task, the "latency to descend" task, and the "latency to cross" task did not differ between the four different groups. Together, these three behavioral tasks provided a well-established method for measuring weekly evolution of sensorimotor coordination and balance following extended ischemic lesion (e.g., cortex and striatum) in rodents over a period of weeks following the initial insult (Matsuura et al., 1997; Carter et al., 2001). Unlesioned sham mice were not affected at any time points, reporting that neither the surgical procedure, the ODN treatment, nor a learning effect interfered in the observations made from MCAO animals. Stroke induced a severe decrease in the ability to execute all three tasks (Fig. 4*C*–*E*), with only a small spontaneous gain of function observed over weeks 1 and 2 in the vehicle-treated group. ODN treatment, however, resulted in a marked improvement on all three task functions, with significance observed by weeks 3 and 4 post-stroke (Fig. 4*C*–*E*). Assessment on two of the three tasks revealed that the MCAO+ODN treatment group was not significantly different compared with unlesioned controls at day 28 post-stroke. ODN had no impact on stroke-induced weight loss, and mortality rate remained similar between ODN- and vehicle-treated groups (Fig. 4*F*). At 28 d post-stroke, brains were collected for further histological analysis. The lesion characteristics (i.e., extent, cavities, and ipsilateral atrophy) revealed no differences between MCAO-vehicle and MCAO-ODN groups, highlighting that ODN treatment was safe when administered from 3 d after the stroke onset (Fig. 4*G*–*I*).

Effect of ODN on functional recovery after photothrombotic stroke

Although the intra-arterial filament occlusion is the gold-standard model for preclinical investigation, a way to strengthen the preclinical evidence of a drug is to challenge it in multiple experimental paradigms. Indeed, the intra-arterial filament occlusion model results in a large corticostriatal infarction, mimicking malignant infarction, while human strokes are mostly small in size. The photothrombotic model produces a small cortical infarction with well-delimited boundaries useful for modeling post-stroke impairments (Corbett et al., 2017). Furthermore, this model is well suited for hydrogel delivery of peptides and small proteins diffusing over several weeks from the stroke cavity into peri-infarct tissue (Overman et al., 2012; Clarkson et al., 2015; Cook et al., 2017). To further differentiate this second model and comply with stroke basic research recommendation (Bernhardt et al., 2017), we used aged female mice (20 ± 2 months) representing a population of stroke sufferers with more severe damage and poorer recovery after the event compared with aged men (Koellhoffer and McCullough, 2013). Hydrogel impregnated with ODN was one-time injected into the infarction cavity 5 d after the onset of stroke (Fig. 5*A*). In this protocol of progressive diffusion from a single depot of gel (7.5 μl), 2 doses of ODN were tested (1 and 5 μg). Photothrombosis produced a well-circumscribed cortical lesion of 3.68 ± 0.43 mm^3 ($n = 5$ mice), as assessed 2 weeks post-stroke, that resulted in some spontaneous

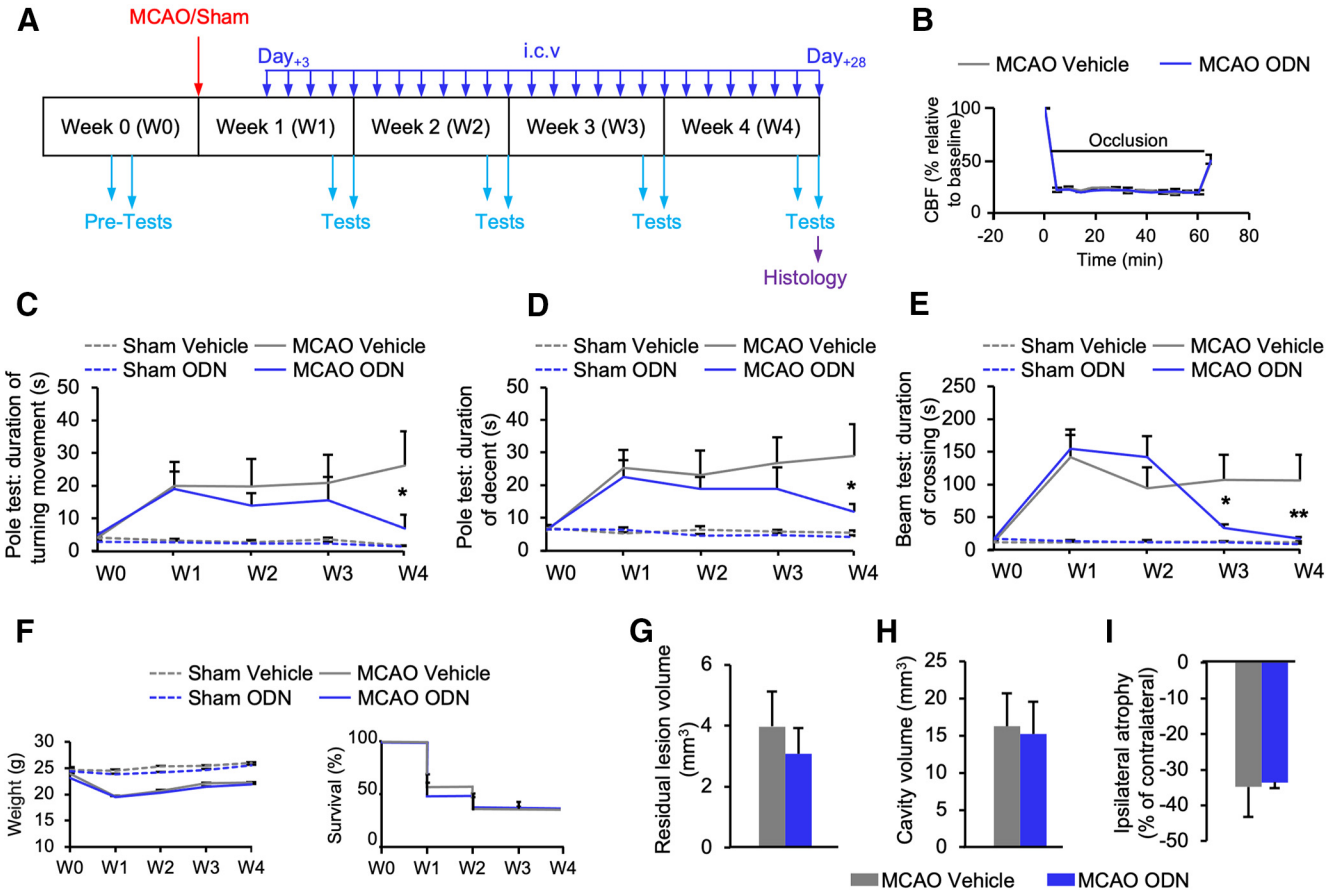

Figure 4. Delayed and chronic treatment with ODN promotes functional recovery after stroke in young adult male mice. ***A***, Timeline diagram of the protocol. Treatment started 3 d after the MCAO procedure (MCAO ODN, $n = 7$; MCAO vehicle, $n = 6$) or the surgery procedure without the MCAO (sham ODN, $n = 6$; and sham vehicle, $n = 6$). ODN or its vehicle was intracerebroventricularly injected every day during the next 25 d (dark blue arrows). Behavioral tests were conducted at the end of each week (light blue arrows). MCAO was similar in the ODN-treated group and the vehicle-treated group (***B***). Mice treated with ODN progressively improved their performances in the execution of (***C***) the turning movement at the top of the vertical pole ($p < 0.05$ at week 4 relative to vehicle-treated animals), (***D***) the descent of the vertical pole ($p < 0.05$ at week 4 relative to vehicle-treated animals), and (***E***) the crossing of the horizontal beam ($p < 0.05$ at week 3 and $p < 0.01$ at week 4 relative to vehicle-treated animals). Sham animals were not sensitive to ODN at any time point, and neither the surgical procedure nor the time affected their performance. Weight loss (***F***, left; $p > 0.05$ vs MCAO+vehicle or Sham+vehicle; MCAO+vehicle, $n = 6$; MCAO+ODN, $n = 7$; Sham+vehicle, $n = 6$; Sham+ODN, $n = 6$) and mortality (***F***, right, Log-rank Mantel–Cox test $p > 0.05$ vs MCAO+vehicle, $n = 6$; MCAO+ODN, $n = 7$) were not different between groups at any time point. At the end of the procedure, histologic analysis of mouse brain showed no difference between groups for the size of the residual lesion (***G***; $p > 0.05$ vs MCAO+vehicle; MCAO+vehicle, $n = 6$; MCAO+ODN, $n = 7$), the total volume of cavities (***H***), and the atrophy of the ipsilateral hemisphere (***I***; $p > 0.05$ vs MCAO+vehicle; MCAO+vehicle, $n = 6$; MCAO+ODN, $n = 7$). Data are mean ± SEM. Data were compared using Mann–Whitney test (***G–I***) or nonparametric two-way ANOVA followed by Bonferroni's *post hoc* testing (***B***, ***F***, left, ***C–E***).

resolution over time with the infarct volume being 2.9 ± 0.6 mm^3 ($n = 10$ mice), as assessed 6 weeks post-stroke at the completion of the behavioral experiments. Treatment with ODN resulted in a dose-dependent decrease in infarct volume ($F_{(2,40)} = 6.74$, $p < 0.003$: ODN (1 µg), 3.44 ± 0.54 mm^3, and 1.86 ± 0.50 mm^3 for weeks 2 and 6, respectively; ODN (5 µg), 2.73 ± 0.84 mm^3, and 1.51 ± 0.39 mm^3; $p < 0.05$, for weeks 2 and 6, respectively; Fig. 5*B*,*C*).

We next tested the mice behaviorally on both the gridwalking (forelimb function) and cylinder (forelimb asymmetry) tasks. Behavioral assessments revealed an increase in the number of footfaults on the gridwalking test ($n = 10$ per group; Fig. 5*D*) and an increase in spontaneous forelimb asymmetry in the cylinder task ($n = 10$ per group; Fig. 5*E*) from 1 week post-stroke. ODN treatment resulted in a dose-dependent decrease in the number of footfaults on the gridwalking task (time effect: $F_{(4,150)} = 33.56$, $p < 0.0001$; treatment effect: $F_{(2,150)} = 28.22$, $p < 0.0001$) and an improvement in forelimb asymmetry in the cylinder task (time effect: $F_{(4,150)} = 48.54$, $p < 0.0001$; treatment effect: $F_{(2,150)} = 18.73$, $p < 0.0001$).

Effects of ODN on modulation of the glial scar

As ODN is a gliopeptide with astrocyte-protective feature (Hamdi et al., 2011), we next investigated whether exogenous administration of ODN has an effect on the glial scar. The glial scar has many roles after a brain ischemia has occurred, both as a regulator of inflammation, but also as a regulator of axonal sprouting and brain excitability, which are critical processes for cortical remapping (Brown et al., 2009; Clarkson et al., 2010; Sofroniew, 2015; Anderson et al., 2016; Lie et al., 2019). We observed a clear upregulation in GFAP expression in the peri-infarct region at both 2 and 6 weeks post-stroke, with expression levels decreasing further away from the stroke border we examined (Fig. 5*F–H*). Chronic treatment with ODN resulted in a dose-dependent decrease in the expression of GFAP in the peri-infarct in both layers 2/3 (both 1 µg, $p < 0.001$; and 5 µg, $p < 0.001$), and 5 (only for 5 µg, $p < 0.001$) as assessed 2 weeks post-stroke (Fig. 5*G*). Assessment of GFAP expression in peri-infarct regions 6 weeks post-stroke revealed no differences in expression between vehicle- and ODN-treated animals in either layers 2/3 or 5 (Fig. 5*H*).

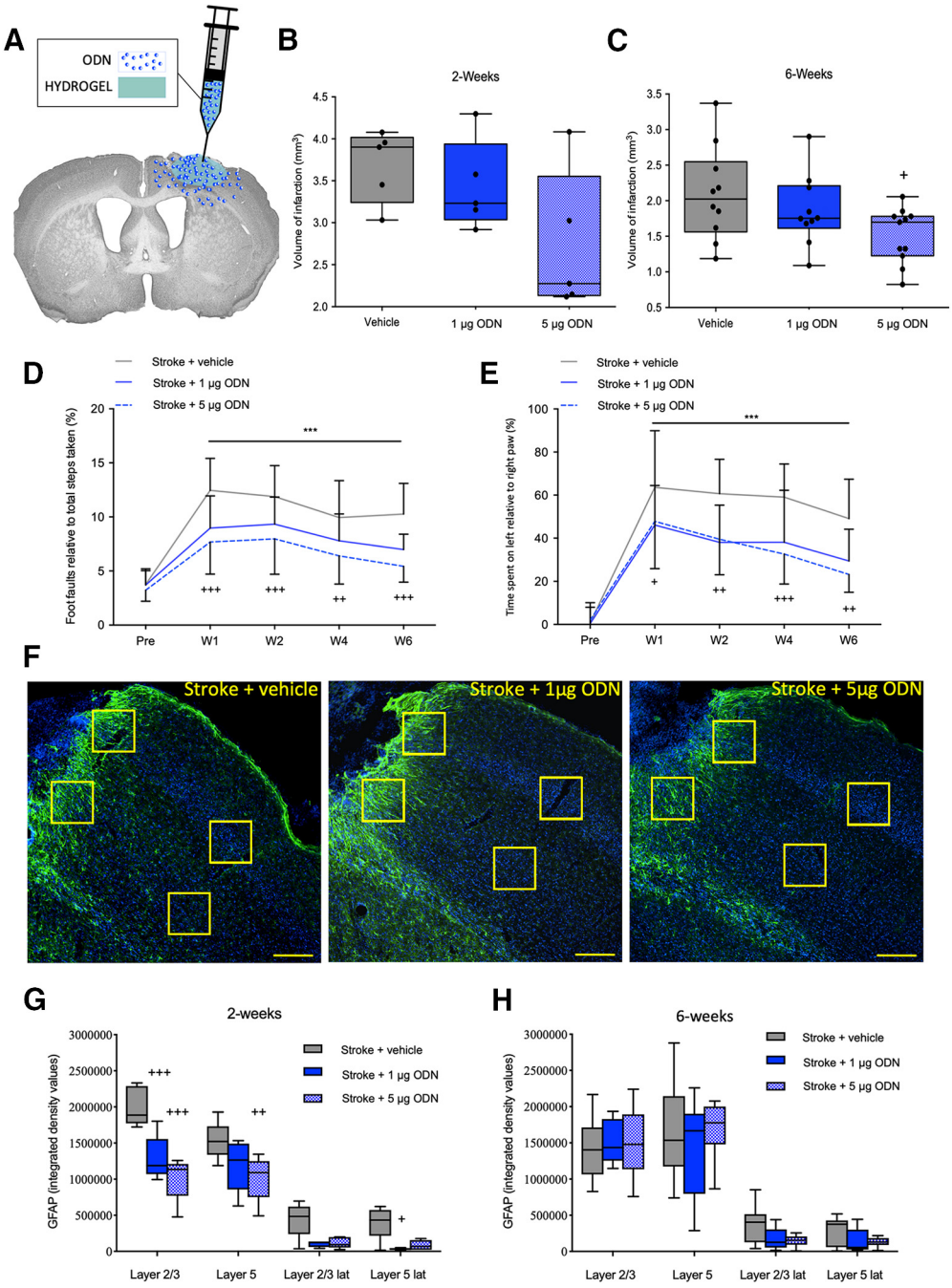

Figure 5. Delayed, chronic treatment with ODN-impregnated hydrogel promotes functional recovery after stroke in aged female mice. ***A***, Schematic illustration of the injectable ODN-impregnated hydrogel. Infarct volume was assessed at 2 (***B***) and 6 (***C***) weeks post-stroke using cresyl violet staining ($n = 5$ and $n = 10$, respectively). Assessment of 1 μg ODN-treated animals showed no differences in infarct volume compared with vehicle-treated controls. However, 5 μg ODN-treated animals exhibited a progressive decrease in stroke volumes with infarct volume being significantly different from vehicle-treated stroke controls 6 weeks post-stroke ($^{+}p < 0.05$; $n = 10$ animals/group). Motor behavioral function was assessed using both the gridwalking (***D***) and cylinder tasks (***E***). On both tasks, ODN (both 1 and 5 μg) resulted in a decrease in the number of footfaults on the gridwalking task and an improvement in forelimb asymmetry in the cylinder task. As ODN is a gliopeptide with astrocyte-protective features, we examined whether ODN treatment affected the extent of peri-infarct glial scarring as assessed by GFAP staining (***F–H***). Representative GFAP- stained sections are shown for stroke + vehicle (***F***, left), stroke + 1 μg ODN (***F***, middle), and stroke + 5 μg ODN (***F***, right) treated animals, 2 weeks post-stroke. Scale bar, 200 μm. GFAP staining intensity was assessed from layers 2/3 and 5, 0-200 μm and 800-1000 μm (each box represents 200 × 200 μm) from the stroke border at 2 (***G***) and 6 weeks (***H***) post-stroke. Treatment with ODN resulted in a dose-dependent decrease in reactive astrogliosis as assessed by GFAP labeling 2 weeks post-stroke (***G***). No differences in GFAP labeling were observed at 6 weeks post-stroke between treatment groups (***H***). $^{+++}p < 0.001$, compared with pre-stroke baseline behavioral controls. $^{+}p < 0.05$, $^{++}p < 0.01$, $^{+++}p < 0.001$, compared with stroke + vehicle controls.

Effects of ODN on tonic inhibitory currents

Given the profile of motor functional recovery, we next sought to investigate the changes in tonic inhibitory currents following treatment with ODN. This is also driven by the fact that we have previously reported that tonic inhibitory currents are elevated from 24 h after stroke and remain elevated for extended period of time due in part to the formation of the glial scar (Clarkson et al., 2010, 2019; Lie et al., 2019). Tonic inhibitory currents were assessed in the peri-infarct cortex of mice after a photothrombotic stroke to the forelimb motor cortex. Layer 2/3 pyramidal

neuron whole-cell voltage-clamp recordings were obtained from brain slices generated *ex vivo* 3-7 d after stroke (Fig. 6*A*,*B*). Recordings obtained 3-7 d after stroke showed an increase in $GABA_AR$-mediated tonic inhibition (control: 53.13 ± 20.04 pA vs stroke: 130.90 ± 39.01 pA; $p < 0.001$; Fig. 6*B*). As ODN is released exclusively by astrocytes, extrasynaptic $GABA_ARs$ receptors are a likely candidate to mediate its effect on neuronal excitability (Tonon et al., 2020). Therefore, we next examined whether bath application of ODN could correct peri-infarct tonic inhibition. Bath application of ODN to slices generated 3-7 d post-stroke resulted in a significant decrease in $GABA_AR$-mediated tonic inhibition (stroke+ODN: 91.25 ± 13.49 pA; $p < 0.05$; Fig. 6*B*) compared with stroke controls. It should be noted, however, that this decrease in tonic inhibitory currents was only a partial reversal with tonic inhibitory currents still significantly elevated compared with sham controls ($p < 0.05$).

Discussion

Studies over recent years have shown that the peri-infarct cortex, which is the tissue adjacent to the stroke, is in a state of heightened plasticity during the subacute period (Murphy and Corbett, 2009). The process of plasticity is highly influenced by $GABA_AR$ signaling and tonic inhibition, which maintains and shapes the level of neuronal excitability (Raimondo et al., 2017). Alteration in GABAergic signaling has been previously reported to be triggered by stroke in both animals and humans (Carmichael, 2012; Johnstone et al., 2018). Accordingly, dampening tonic inhibitory currents using a NAM targeting α_5-containing $GABA_ARs$ from 3-7 d post-stroke, but not acutely within hours, increases motor functional recovery in animal stroke models (Clarkson et al., 2010; Lake et al., 2015). Consistent with these observations, the present findings demonstrate that exogenous administration of ODN enhances cortical excitability in a magnitude that makes it toxic when administered during the acute stage of stroke (within hours of stroke onset) and, however, makes it instrumental to safely boost functional recovery when administered during the subacute (3-7 d) recovery stages of stroke.

The endozepine, ODN, has been repeatedly categorized as a $GABA_AR$ NAM (Bormann et al., 1985; Costa and Guidotti, 1991; Alfonso et al., 2012; Dumitru et al., 2017). Yet, all these experiments have been conducted *in vitro*. Here, we report, for the first time, *in vivo*, that ODN increases cortical neuronal activity and excitability. Interestingly, we also report that astrocytes respond to the treatment. The question of whether this activation is a consequence of neuronal activity or a direct effect on astrocytes, as previously found in cell culture, remains unclear (Gach et al., 2015). However, it is possible that ODN works on both systems as we reported herein that administration of ODN partially dampens both the stroke-induced elevation in tonic inhibitory currents as well as the level of reactive astrogliosis in the peri-infarct cortex.

Capitalizing on our confirmation of ODN as an enhancer of cortical excitability, we assessed the effect of a gain or loss of ODN during the acute phase of brain ischemia/reperfusion. In line with our predictions, when ODN was administered during brain ischemia, cerebral damage was dramatically increased. In addition, the finding that $DBI^{-/-}$ mice were less vulnerable to transient focal ischemia than WT mice suggests that even the endogenous production of DBI (and therefore ODN) during stroke is deleterious.

In the acute stage of stroke, minor changes in various physiological and metabolic parameters can have major consequences

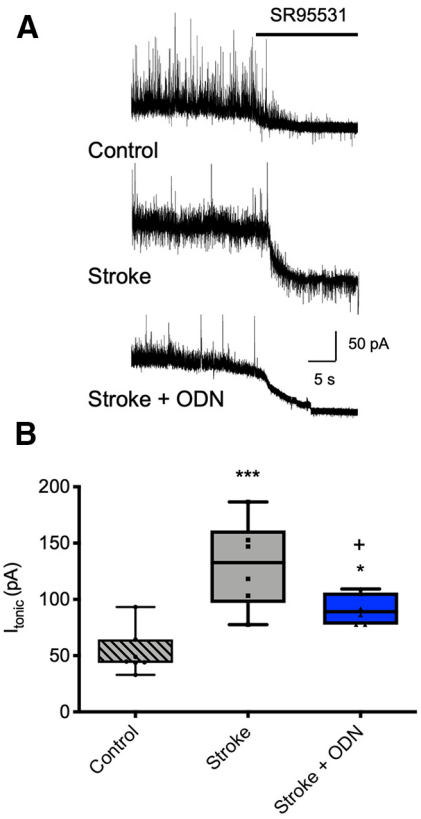

Figure 6. ODN dampens the stroke-induced elevation in tonic $GABA_AR$ currents in layer 2/3 pyramidal neurons. Whole-cell patch-clamp recordings were made from post-stroke brain slices, within 500 μm of infarct, from layer 2/3 pyramidal neurons. Representative traces showing the tonic inhibitory currents in control ($n = 7$), stroke ($n = 6$), and stroke + ODN ($n = 6$) treated animals (***A***). Tonic currents were revealed by the shift in holding currents after blocking all $GABA_ARs$ with gabazine (SR95531; 100 μM). Box plot (whiskers, minimum and maximum; lines, median) represents an increase in tonic inhibitory currents in peri-infarct cortical neurons that is partially dampened following exposure to ODN (***B***). Horizontal bar represents the application of the $GABA_AR$ antagonist, SR95531. Cells were voltage-clamped at 10 mV. $^*p < 0.05$, $^{***}p < 0.001$, compared with tonic currents from control animal. $^+p < 0.05$, compared with tonic currents from stroke animal.

on tissue viability. We first verified that i.c.v. administration of ODN did not change body temperature, food intake, or cardiovascular activity. Second, it should be noted that ODN is not pro-apoptotic or pro-inflammatory (Hamdi et al., 2011; Kaddour et al., 2013). Third, although the quality of the brain microcirculation is critical in the penumbra, we did not find any evidence of a vasomotor activity of ODN, such as vasoconstrictions of brain arteries (our personal observations). Although $GABA_ARs$ are expressed in many cell types, only those containing the $\gamma 2$ subunit can bind benzodiazepines and potentially ODN. Indeed, this subunit is very frequent in neurons but weakly or not expressed in oligodendrocytes, microglia, astrocytes, and endothelial cells of adult brain mice (Cahoy et al., 2008). We are left, then, with a primary effect of ODN on inhibitory transmission and the most parsimonious explanation for why ODN exacerbated the cellular damage following stroke is because of an increase in neuronal excitation. This is in line with the effect of the $GABA_AR$ NAM L655,708 when used too early after a cortical ischemia (Clarkson et al., 2010). In support of this view, we report here that ODN exacerbates NMDA-induced excitotoxic damages. We also show that ODN increases the number of spreading depolarization waves. The trigger of spreading depolarization waves is actually settled over the level of neuronal

excitation, and their propagation out from the site of infarction is known to be a leading cause of ischemic infarct growth (Chuquet et al., 2007; von Bornstädt et al., 2015). Therefore, for neurons at immediate threat of death during the acute phase (<3 d), ODN may amplify the depolarization and lead to an irreversible calcium overload. Our results indicate that there is a need to develop specific endozepine blockers to prevent their action on $GABA_A$Rs during the acute phase of cerebral ischemia.

To date, no NAMs that target the benzodiazepine-binding site to reduce GABAergic activity and that lack any proconvulsant or anxiogenic effects are available for clinical use. However, clinical trials using α5-containing $GABA_A$R NAMs for enhancing stroke recovery are being explored in phase II trials (www.ClinicalTrials.gov: Hoffman La-Roche, NCT02928393; Servier RESTORE BRAIN Study, NCT02877615). It is increasingly recognized that GABAergic NAMs used at a safe dosage and that target specific subunit compositions will be therapeutically useful, for example, to improve cognitive functions in brain conditions where diminished excitability has to be boosted (Bolognani et al., 2015; Soh and Lynch, 2015). There is also growing evidence that impairment in GABA transporter (GAT-3/GAT-4) function contributes to the peri-infarct zone changes in neuronal inhibition and post-stroke functional recovery (Clarkson et al., 2010; Carmichael, 2012). As a consequence, the excessive GABAergic tone inhibits sensorimotor recovery and is likely due in part to synaptic plasticity and LTP, being suboptimal (Atack et al., 2006). Two independent studies have demonstrated that the use of a benzodiazepine site-specific NAM improves post-stroke motor recovery in adult males (Clarkson et al., 2010; Lake et al., 2015). In addition, a recent study showed that the treatment with the GAT3 substrate, L-isoserine, administered directly into the stroke cavity, can increase GAT3 expression and improve functional recovery after focal ischemic stroke (Lie et al., 2019). Following this idea and protocol, we found that daily administration of ODN started 3 d after ischemia or hydrogel delivery from 5 d (i.e., when the risk of ODN-induced cell death had ceased) remarkably improved motor coordination. Of note, the precursor of ODN, DBI, is one of the most transcripted genes in astrocytes (Zhang et al., 2014). The fact that GABA inhibits the release of ODN by astrocytes (Patte et al., 1999) suggests that, in the neighborhood of the stroke lesion, the excess in ambient GABA is likely preventing sufficient endozepine production.

This functional recovery cannot be because of a difference in stroke severity between groups for the three following reasons: (1) the average decrease of blood flow was identical over the 60 min of ischemia, (2) the mean brain histologic sequelae were similar at day 28, and (3) the mortality rate had the same kinetics in both groups. Moreover, ODN-treated animals did not display any obvious behavior indicative of anxiety, aggression, or hyperactivity, suggesting that both the timing and dose of ODN administered led to a safe and efficient treatment to promote functional recovery.

To date, all translational studies have failed to treat stroke in part because preclinical studies routinely failed to use clinically relevant animal models. Several recommendations have been made, among which was the use of aged animals of both sexes since aging remains the major nonmodifiable risk factor for stroke (Jolkkonen and Kwakkel, 2016; Corbett et al., 2017). Aged females represent the greatest percentage of stroke sufferers, with strokes in this population being more severe and recovery being worse than males and younger females (Koellhoffer and McCullough 2013). Therefore, to challenge ODN efficacy and increase the translational value of our results, we studied the effect of ODN in a radically different experimental paradigm. Using the photothrombotic model of ischemia in aged female mice, we obtained a small infarction circumscribed to the cortex. We took advantage of the topology of the lesion to also test whether a single depot of ODN into the infarction cavity on day 5 post-stroke would improve functional recovery. Although the number of new peptides entering clinical trials continues to grow, their therapeutic potential in neurology has not yet been realized because they rarely get through the blood–brain barrier and their half-life *in vivo* limits the time window to exert their action (Penchala et al., 2015). Hydrogel impregnated with peptides or small proteins has been extensively used as a system of chronical delivery (for review, see Fernandez-Serra et al., 2020). Specifically, we and others have shown that biomolecules embedded into hydrogels have a sustained, consistent release into surrounding tissue lasting ~3-4 weeks (Tae et al., 2006; Li et al., 2010; Overman et al., 2012; Clarkson et al., 2015; Cook et al., 2017). For instance, cyclosporin, an 11-amino acid-long peptide of 1.2 kDa (i.e., similar to ODN, 18-residue-long for 1.9 kDa) is slowly released by the hydrogel in a 2 mm cortical zone around the gel for at least 24 d (Tuladhar et al., 2015). Therefore, the hydrogel provides a protective micro-environment for ODN and allows its controlled delivery around the lesion, where excitability needs to be enhanced. In this second stroke model, ODN was able to improve sensorimotor task performance as soon as week 1. These studies highlight a novel example for hydrogel delivery systems offering a support for effective peptide biodisponibility that bypasses the blood–brain barrier to achieve consistent recovery post-stroke. Although 1 μg was effective in the MCAO protocol, only the dose of 5 μg was effective in the photothrombotic protocol. This is not surprising considering that, in the MCAO protocol, a daily dose of 1 μg was administered, while in the photothrombotic protocol, ODN was delivered to the peri-infarct cortex from a single depot of hydrogel. Furthermore, others have also observed that, when hydrogel is used to vehiculate a bioactive molecule in the brain, such as neurotrophins, a higher quantity of the latter is necessary (Ravina et al., 2018).

Overall, our data are strikingly reminiscent of the findings of others (Clarkson et al., 2010; Lake et al., 2015). Using a small naturally occurring peptide that is expressed and released by astrocytes and known to act as a $GABA_A$R NAM, we found the same versatile effect in stroke as with the synthetic $GABA_A$R NAM, L655-708: deleterious in the acute phase but promotor of recovery in the chronic phase. L655-708 is an imidazobenzodiazepine selective for the extrasynaptic $GABA_A$R that contains the benzodiazepine-sensitive subunit α_5 and, as an inverse agonist, reduces the tonic inhibition. Interestingly, L655-708 has been shown to facilitate LTP by shifting toward less inhibitory activity (Atack et al., 2006). Similarly, we found that ODN was able to dampen the ambient tonic inhibition surrounding the stroke lesion. This disinhibition may be permissive for plastic rearrangements in the peri-infarct cortex to occur (Ziemann et al., 2001; Cicinelli et al., 2003; Clarkson and Carmichael, 2009). Therefore, one hypothesis requiring future attention is that ODN selectively binds to α_5-containing $GABA_A$R. It is also possible that these changes in tonic inhibitory currents occur through changes in presynaptic GABA signaling or astrocytic function, which is another two suggested pathways that need to be explored in future experiments. In parallel, another possible mechanism that needs to be examined is neurogenesis. The group of Monyer have recently shown that ODN reduces the GABA-mediated current of neural stem/progenitor cell of the subventricular, inducing their proliferation and migration (Alfonso et al., 2012; Dumitru et al., 2017),

supporting a role of endozepines in neurogenesis. Additional work should be undertaken to test the hypothesis that poststroke neurogenesis can be controlled by ODN to optimize functional recovery.

The modification of network connections and synaptic strength allowing functional recovery requires that homeostatic mechanisms, such as the maintenance of excitation/inhibition balance at the network, single-cell, and synapse level, be in their operating range (Buzsáki, 2007). Our results suggest that endozepines play a significant role to tuning this balance and reinforce the idea that an appropriate correction of GABAergic tone at the right time can facilitate functional recovery after stroke.

References

Alfonso J, Le Magueresse C, Zuccotti A, Khodosevich K, Monyer H (2012) Diazepam binding inhibitor promotes progenitor proliferation in the post-natal SVZ by reducing GABA signaling. Cell Stem Cell 10:76–87.

Alia C, Spalletti C, Lai S, Panarese A, Micera S, Caleo M (2016) Reducing $GABA_A$-mediated inhibition improves forelimb motor function after focal cortical stroke in mice. Sci Rep 6:37823.

Anderson MA, Burda JE, Ren Y, Ao Y, O'Shea TM, Kawaguchi R, Coppola G, Khakh BS, Deming TJ, Sofroniew MV (2016) Astrocyte scar formation aids central nervous system axon regeneration. Nature 532:195–200.

Atack JR, Bayley PJ, Seabrook GR, Wafford KA, McKernan RM, Dawson GR (2006) L-655,708 enhances cognition in rats but is not proconvulsant at a dose selective for alpha5-containing $GABA_A$ receptors. Neuropharmacology 51:1023–1029.

Bachtiar V, Stagg CJ (2014) The role of inhibition in human motor cortical plasticity. Neuroscience 278:93–104.

Barmack NH, Bilderback TR, Liu H, Qian Z, Yakhnitsa V (2004) Activity-dependent expression of acyl-coenzyme a-binding protein in retinal Müller glial cells evoked by optokinetic stimulation. J Neurosci 24:1023–1033.

Bernhardt J, Hayward KS, Kwakkel G, Ward NS, Wolf SL, Borschmann K, Krakauer JW, Boyd LA, Carmichael ST, Corbett D, Cramer SC (2017) Agreed definitions and a shared vision for new standards in stroke recovery research: the stroke recovery and rehabilitation roundtable taskforce. Neurorehabil Neural Repair 31:793–799.

Bolognani F, Squassante L, Liogier d'Ardhuy X, Hernandez MC, Knoflach F, Baldinotti I (2015) RG1662, a selective $GABA_A$ $\alpha5$ receptor negative allosteric modulator, increases gamma power in young adults with down syndrome. Neurology 84:273.

Bormann J (1991) Electrophysiological characterization of diazepam binding inhibitor (DBI) on $GABA_A$ receptors. Neuropharmacology 30:1387–1389.

Bormann J, Ferrero P, Guidotti A, Costa E (1985) Neuropeptide modulation of GABA receptor $C1^-$ channels. Regul Pept Suppl 4:33–38.

Brown CE, Aminoltejari K, Erb H, Winship IR, Murphy TH (2009) In vivo voltage-sensitive dye imaging in adult mice reveals that somatosensory maps lost to stroke are replaced over weeks by new structural and functional circuits with prolonged modes of activation within both the peri-infarct zone and distant sites. J Neurosci 29:1719–1734.

Buzsáki G (2007) Rhythms of the brain. New York: Oxford UP.

Cahoy JD, Emery B, Kaushal A, Foo LC, Zamanian JL, Christopherson KS, Xing Y, Lubischer JL, Krieg PA, Krupenko SA, Thompson WJ, Barres BA (2008) A transcriptome database for astrocytes, neurons, and oligodendrocytes: a new resource for understanding brain development and function. J Neurosci 28:264–278.

Carmichael ST (2012) Brain excitability in stroke: the yin and yang of stroke progression. Arch Neurol 69:161–167.

Carter RJ, Morton J, Dunnett SB (2001) Motor coordination and balance in rodents. Curr Protoc Neurosci 8:8–12.

Chuquet J, Hollender L, Nimchinsky EA (2007) High-resolution in vivo imaging of the neurovascular unit during spreading depression. J Neurosci 27:4036–4044.

Chuquet J, Quilichini P, Nimchinsky EA, Buzsáki G (2010) Predominant enhancement of glucose uptake in astrocytes versus neurons during activation of the somatosensory cortex. J Neurosci 30:15298–15303.

Cicinelli P, Pasqualetti P, Zaccagnini M, Traversa R, Oliveri M, Rossini PM (2003) Interhemispheric asymmetries of motor cortex excitability in the postacute stroke stage: a paired-pulse transcranial magnetic stimulation study. Stroke 34:2653–2658.

Clarkson AN, Boothman-Burrell L, Dósa Z, Nagaraja RY, Jin L, Parker K, van Nieuwenhuijzen PS, Neumann S, Gowing EK, Gavande N, Ahring PK, Holm MM, Hanrahan JR, Nicolazzo JA, Jensen K, Chebib M (2019) The flavonoid, 2′-methoxy-6-methylflavone, affords neuroprotection following focal cerebral ischaemia. J Cereb Blood Flow Metab 39:1266–1282.

Clarkson AN, Carmichael ST (2009) Cortical excitability and post-stroke recovery. Biochem Soc Trans 37:1412–1414.

Clarkson AN, Huang BS, Macisaac SE, Mody I, Carmichael ST (2010) Reducing excessive GABA-mediated tonic inhibition promotes functional recovery after stroke. Nature 468:305–309.

Clarkson AN, Overman JJ, Zhong S, Mueller R, Lynch G, Carmichael ST (2011) AMPA receptor-induced local brain-derived neurotrophic factor signaling mediates motor recovery after stroke. J Neurosci 31:3766–3775.

Clarkson AN, Parker K, Nilsson M, Walker FR, Gowing EK (2015) Combined ampakine and BDNF treatments enhance poststroke functional recovery in aged mice via AKT-CREB signaling. J Cereb Blood Flow Metab 35:1272–1279.

Cook DJ, Nguyen C, Chun HN, Llorente I, Chiu AS, Machnicki M, Zarembinski TI, Carmichael ST (2017) Hydrogel-delivered brain-derived neurotrophic factor promotes tissue repair and recovery after stroke. J Cereb Blood Flow Metab 37:1030–1045.

Corbett D, Carmichael ST, Murphy TH, Jones TA, Schwab ME, Jolkkonen J, Clarkson AN, Dancause N, Weiloch T, Johansen-Berg H, Nilsson M, McCullough LD, Joy MT (2017) Enhancing the alignment of the preclinical and clinical stroke recovery research pipeline: consensus-based core recommendations from the Stroke Recovery and Rehabilitation Roundtable Translational Working Group. Neurorehabil Neural Repair 31:699–707.

Costa E, Guidotti A (1991) Diazepam binding inhibitor (DBI): a peptide with multiple biological actions. Life Sci 49:325–344.

Dumitru I, Neitz A, Alfonso J, Monyer H (2017) Diazepam binding inhibitor promotes stem cell expansion controlling environment-dependent neurogenesis. Neuron 94:125–137.

Fernandez-Serra R, Gallego R, Lozano P, González-Nieto D (2020) Hydrogels for neuroprotection and functional rewiring: a new era for brain engineering. Neural Regen Res 15:783–789.

Ferrero P, Santi MR, Conti-Tronconi B, Costa E, Guidotti A (1986) Study of an octadecaneuropeptide derived from diazepam binding inhibitor (DBI): biological activity and presence in rat brain. Proc Natl Acad Sci USA 83:827–831.

Gach K, Belkacemi O, Lefranc B, Perlikowski P, Masson J, Walet-Balieu ML, Do-Rego JC, Galas L, Schapman D, Lamtahri R, Tonon MC, Vaudry D, Chuquet J, Leprince J (2015) Detection, characterization and biological activities of [bisphospho-Thr3,9]ODN, an endogenous molecular form of ODN released by astrocytes. Neuroscience 290:472–484.

Galeffi F, Sinnar S, Schwartz-Bloom RD (2000) Diazepam promotes ATP recovery and prevents cytochrome C release in hippocampal slices after in vitro ischemia. J Neurochem 75:1242–1249.

Green AR, Hainsworth AH, Jackson DM (2000) GABA potentiation: a logical pharmacological approach for the treatment of acute ischaemic stroke. Neuropharmacology 39:1483–1494.

Guidotti A, Forchetti CM, Corda MG, Konkel D, Bennett CD, Costa E (1983) Isolation, characterization, and purification to homogeneity of an endogenous polypeptide with agonistic action on benzodiazepine receptors. Proc Natl Acad Sci USA 80:3531–3535.

Hamdi Y, Masmoudi-Kouki O, Kaddour H, Belhadj F, Gandolfo P, Vaudry D, Mokni M, Leprince J, Hachem R, Vaudry H, Tonon MC, Amri M (2011) Protective effect of the octadecaneuropeptide on hydrogen peroxide-induced oxidative stress and cell death in cultured rat astrocytes. J Neurochem 118:416–428.

Hartings JA, Shuttleworth CW, Kirov SA, Ayata C, Hinzman JM, Foreman B, Andrew RD, Boutelle MG, Brennan KC, Carlson AP, Dahlem MA, Drenckhahn C, Dohmen C, Fabricius M, Farkas E, Feuerstein D, Graf R, Helbok R, Lauritzen M, Major S et al., (2017) The continuum of spreading depolarizations in acute cortical lesion development: Examining Leão's legacy. J Cereb Blood Flow Metab 37:1571–1594.

Houlton J, Zhou LY, Barwick D, Gowing EK, Clarkson AN (2019) Stroke induces a BDNF-dependent improvement in cognitive flexibility in aged mice. Neural Plast 2019:1460890.

Hummel FC, Steven B, Hoppe J, Heise K, Thomalla G, Cohen LG, Gerloff C (2009) Deficient intracortical inhibition (SICI) during movement preparation after chronic stroke. Neurology 72:1766–1772.

Johnstone A, Levenstein JM, Hinson EL, Stagg CJ (2018) Neurochemical changes underpinning the development of adjunct therapies in recovery after stroke: a role for GABA? J Cereb Blood Flow Metab 38:1564–1583.

Jolkkonen J, Kwakkel G (2016) Translational hurdles in stroke recovery studies. Transl Stroke Res 7:331–342.

Kaddour H, Hamdi Y, Vaudry D, Basille M, Desrues L, Leprince J, Castel H, Vaudry H, Tonon MC, Amri M, Masmoudi-Kouki O (2013) The octadecaneuropeptide ODN prevents 6-hydroxydopamine-induced apoptosis of cerebellar granule neurons through a PKC-MAPK-dependent pathway. J Neurochem 125:620–633.

Kim YK, Yang EJ, Cho K, Lim JY, Paik NJ (2014) Functional recovery after ischemic stroke is associated with reduced GABAergic inhibition in the cerebral cortex: a GABA PET study. Neurorehabil Neural Repair 28:576–583.

Koellhoffer EC, McCullough LD (2013) The effects of estrogen in ischemic stroke. Transl Stroke Res 4:390–401.

Lake EM, Chaudhuri J, Thomason L, Janik R, Ganguly M, Brown M, McLaurin J, Corbett D, Stanisz GJ, Stefanovic B (2015) The effects of delayed reduction of tonic inhibition on ischemic lesion and sensorimotor function. J Cereb Blood Flow Metab 35:1601–1609.

Leprince J, Oulyadi H, Vaudry D, Masmoudi O, Gandolfo P, Patte C, Costentin J, Fauchère JL, Davoust D, Vaudry H, Tonon MC (2001) Synthesis, conformational analysis and biological activity of cyclic analogs of the octadecaneuropeptide ODN: design of a potent endozepine antagonist. Eur J Biochem 268:6045–6057.

Li S, Overman JJ, Katsman D, Kozlov SV, Donnelly CJ, Twiss JL, Giger RJ, Coppola G, Geschwind DH, Carmichael ST (2010) An age-related sprouting transcriptome provides molecular control of axonal sprouting after stroke. Nat Neurosci 13:1496–1504.

Lie ME, Gowing EK, Johansen NB, Dalby NO, Thiesen L, Wellendorph P, Clarkson AN (2019) GAT3 selective substrate L-isoserine upregulates GAT3 expression and increases functional recovery after a focal ischemic stroke in mice. J Cereb Blood Flow Metab 39:74–88.

Loomis WF, Behrens MM, Williams ME, Anjard C (2010) Pregnenolone sulphate and cortisol induce secretion of acyl-CoA-binding protein and its conversion into endozepines from astrocytes. J Biol Chem 285:21359–21365.

Mann A, Chesselet MF (2014) Techniques for motor assessment in rodent. In: Movement disorders, genetics and models, Ed 2 (LeDoux M, ed), pp 139–157. Amsterdam: Elsevier.

Marshall JW, Green AR, Ridley RM (2003) Comparison of the neuroprotective effect of clomethiazole, AR-R15896AR and NXY-059 in a primate model of stroke using histological and behavioural measures. Brain Res 972:119–126.

Matsuura K, Kabuto H, Makino H, Ogawa N (1997) Pole test is a useful method for evaluating the mouse movement disorder caused by striatal dopamine depletion. J Neurosci Methods 73:45–48.

Möhler H (2014) Endogenous benzodiazepine site peptide ligands operating bidirectionally in vivo in neurogenesis and thalamic oscillations. Neurochem Res 39:1032–1036.

Murphy TH, Corbett D (2009) Plasticity during stroke recovery: from synapse to behaviour. Nat Rev Neurosci 10:861–872.

Neess D, Bloksgaard M, Bek S, Marcher AB, Elle IC, Helledie T, Due M, Pagmantidis V, Finsen B, Wilbertz J, Kruhøffer M, Færgeman N, Mandrup S (2011) Disruption of the acyl-CoA binding protein gene delays hepatic adaptation to metabolic changes at weaning. J Biol Chem 286:3460–3472.

Orfila JE, Grewal H, Dietz RM, Strnad F, Shimizu T, Moreno M, Schroeder C, Yonchek J, Rodgers KM, Dingman A, Bernard TJ, Quillinan N, Macklin WB, Traystman RJ, Herson PS (2019) Delayed inhibition of tonic inhibition enhances functional recovery following experimental ischemic stroke. J Cereb Blood Flow Metab 39:1005–1014.

Overman JJ, Clarkson AN, Wanner IB, Overman WT, Eckstein I, Maguire JL (2012) A role for ephrin-A5 in axonal sprouting, recovery, and activity-dependent plasticity after stroke. Proc Natl Acad Sci USA 109:2230–2239.

Patte C, Gandolfo P, Leprince J, Thoumas JL, Fontaine M, Vaudry H, Tonon MC (1999) GABA inhibits endozepine release from cultured rat astrocytes. Glia 25:404–411.

Penchala SC, Miller MR, Pal A, Dong J, Madadi NR, Xie J, Joo H, Tsai J, Batoon P, Samoshin V, Franz A, Cox T, Miles J, Chan WK, Park MS, Alhamadsheh MM (2015) A biomimetic approach for enhancing the in vivo half-life of peptides. Nat Chem Biol 11:793–798.

Qian Z, Bilderback TR, Barmack NH (2008) Acyl coenzyme A-binding protein (ACBP) is phosphorylated and secreted by retinal Müller astrocytes following protein kinase C activation. J Neurochem 105:1287–1299.

Raimondo JV, Richards BA, Woodin MA (2017) Neuronal chloride and excitability: the big impact of small changes. Curr Opin Neurobiol 43:35–42.

Ravina K, Briggs D, Kislal S, Warraich Z, Nguyen T, Lam R, Zarembinski T, Shamloo M (2018) Intracerebral delivery of brain-derived neurotrophic factor using HyStem®-C hydrogel implants improves functional recovery and reduces neuroinflammation in a rat model of ischemic stroke. Int J Mol Sci 19:3782–3794.

Rossant C, Kadir SN, Goodman DF, Schulman J, Hunter ML, Saleem AB, Grosmark A, Belluscio M, Denfield GH, Ecker AS, Tolias AS, Solomon S, Buzsaki G, Carandini M, Harris KD (2016) Spike sorting for large, dense electrode arrays. Nat Neurosci 19:634–641.

Roux L, Buzsáki G (2015) Tasks for inhibitory interneurons in intact brain circuits. Neuropharmacology 88:10–23.

Schwartz RD, Huff RA, Yu X, Carter ML, Bishop M (1994) Post-ischemic diazepam is neuroprotective in the gerbil hippocampus. Brain Res 647:153–160.

Schwartz RD, Yu X, Katzman MR, Hayden-Hixson DM, Perry JM (1995) Diazepam, given post-ischemia, protects selectively vulnerable neurons in the rat hippocampus and striatum. J Neurosci 15:529–539.

Schwartz-Bloom RD, Sah R (2001) Gamma-aminobutyric acid (A) neurotransmission and cerebral ischemia. J Neurochem 77:353–371.

Schwartz-Bloom RD, McDonough KJ, Chase PJ, Chadwick LE, Inglefield JR, Levin ED (1998) Long-term neuroprotection by benzodiazepine full versus partial agonists after transient cerebral ischemia in the gerbil. J Cereb Blood Flow Metab 18:548–558.

Shuaib A, Kanthan R (1997) Amplification of inhibitory mechanisms in cerebral ischemia: an alternative approach to neuronal protection. Histol Histopathol 12:185–194.

Sofroniew MV (2015) Astrocyte barriers to neurotoxic inflammation. Nat Rev Neurosci 16:249–263.

Soh MS, Lynch JW (2015) Selective modulators of α5-containing $GABA_A$ receptors and their therapeutic significance. Curr Drug Targets 16:735–746.

Sydserff SG, Cross AJ, Green AR (1995) The neuroprotective effect of chlormethiazole on ischaemic neuronal damage following permanent middle cerebral artery ischaemia in the rat. Neurodegeneration 4:323–328.

Tae G, Scatena M, Stayton PS, Hoffman AS (2006) PEG-cross-linked heparin is an affinity hydrogel for sustained release of vascular endothelial growth factor. J Biomater Sci Polym Ed 17:187–197.

Tonon MC, Vaudry H, Chuquet J, Guillebaud F, Fan J, Masmoudi-Kouki O, Vaudry D, Lanfray D, Morin F, Prevot V, Papadopoulos V, Troadec JD, Leprince J (2020) Endozepines and their receptors: structure, functions and pathophysiological significance. Pharmacol Ther 208:107386.

Tuladhar A, Morshead CM, Shoichet MS (2015) Circumventing the blood-brain barrier: local delivery of cyclosporin A stimulates stem cells in stroke-injured rat brain. J Control Release 215:1–11.

Vezzani A, Serafini R, Stasi MA, Samanin R, Ferrarese C (1991) Epileptogenic activity of two peptides derived from diazepam binding inhibitor after intrahippocampal injection in rats. Epilepsia 32:597–603.

von Bornstädt D, Houben T, Seidel JL, Zheng Y, Dilekoz E, Qin T, Sandow N, Kura S, Eikermann-Haerter K, Endres M, Boas DA, Moskowitz MA, Lo EH, Dreier JP, Woitzik J, Sakadzõić S, Ayata C (2015) Supply-demand mismatch transients in susceptible peri-infarct hot zones explain the origins of spreading injury depolarizations. Neuron 85:1117–11131.

Zhang Y, Chen K, Sloan SA, Bennett ML, Scholze AR, O'Keeffe S, Phatnani HP, Guarnieri P, Caneda C, Ruderisch N, Deng S, Liddelow SA, Zhang C, Daneman R, Maniatis T, Barres BA, Wu JQ (2014) An RNA-sequencing transcriptome and splicing database of glia, neurons, and vascular cells of the cerebral cortex. J Neurosci 34:11929–11947.

Ziemann U, Muellbacher W, Hallett M, Cohen LG (2001) Modulation of practice-dependent plasticity in human motor cortex. Brain 124:1171–1181.